Received: 25 February 2021 | Revised: 12 April 2021 | Accepted: 13 April 2021

DOI: 10.1002/jlcr.3910

RESEARCH ARTICLE

Journal of Labelled Compounds and Radiopharmaceuticals WILEY

Preparation and biological evaluation of radioiodine-labeled triphenylphosphine derivatives as mitochondrial targeting probes

Shuyu Shi[1,2] | **Zelan Liu**[1,2] | **Zhenmin Wu**[1,2] | **Hang Zhou**[1,2] | **Jie Lu**[1,2]

[1]Key Laboratory of Radiopharmaceuticals, Beijing Normal University, Ministry of Education, Beijing, China

[2]College of Chemistry, Beijing Normal University, Beijing, China

Correspondence
Jie Lu, Key Laboratory of Radiopharmaceuticals, Beijing Normal University, Ministry of Education; or College of Chemistry, Beijing Normal University, Beijing 100875, China.
Email: ljie74@bnu.edu.cn

Funding information
National Natural Science Foundation of China, Grant/Award Number: 21976019

The positive-charged lipophilic triphenylphosphonium cations ($TPPs^+$) have been served as mitochondrial targeting vehicles for the delivery of various probes. In this study, we developed a new method for the preparation of radioiodine-labeled $TPPs^+$. Four ^{125}I-labeled $TPPs^+$, **[^{125}I] 9–[^{125}I] 12**, were prepared from the corresponding triphenylphosphine phenylborate precursors of **B 5–B 8** via an optimized copper-catalyzed one-step procedure in high radiochemical yield (>95%). After radio-HPLC purification, the final products could be obtained with high specific activity. Their physicochemical properties, in vitro cellular uptake, and ex vivo mice biodistribution were investigated. The results suggested the ^{125}I-labeled $TPPs^+$ were lipophilic and could specifically accumulate in the mitochondrial-rich myocardial cells through the mitochondrial membrane potential.

KEYWORDS
^{125}I, copper-catalyzed radioiodination, mitochondrial membrane potential, triphenylphosphonium cations

1 | INTRODUCTION

Mitochondria are recognized as the powerhouse of the cell. Their central function is the synthesis of ATP by oxidative phosphorylation.[1] Mitochondrial dysfunction can lead to a wide range of debilitating or life-threatening diseases such as cancer, heart failure, and neurodegenerative diseases.[2–5] Therefore, mitochondria are regarded as an important target for early diagnosis and treatment of these diseases.

However, the highly hydrophobic inner membrane and negative membrane potential of mitochondria result in limited diffusive transport. The majority of mitochondria-targeted probes commonly contain lipophilic, cationic moieties, including dequalinium (DQA), rhodamine, triphenyl phosphonium cations ($TPPs^+$), and peptide sequences.[6] Among them, the $TPPs^+$ contain three phenyl groups, which make the whole molecule highly lipid soluble. In addition, the positive charge on the phosphorus atom can be delocalized to the three benzene rings. These properties make it easy for $TPPs^+$ to pass through phospholipid bilayers into the cytoplasm bilayers by passive diffusion.[7–9] Driven by the mitochondrial membrane potential ($\Delta\Psi$), $TPPs^+$ can be further accumulated from the cytoplasm into mitochondria. The uptake of lipophilic cations into mitochondria increases 10-fold for every 61.5 mV of membrane potential at 37°C, which lead to 100- to 500-fold accumulation of $TPPs^+$ within mitochondria.[6] Thus, $TPPs^+$ have been used to attach to various small molecules for the diagnosis or treatment of these cancer and cardiovascular disease, such as the antioxidants quinone,[10] Vitamin E,[11] and ebselen,[12] as well as the radionuclides.[13–15]

Despite the widespread clinical applications of ^{99m}Tc-MIBI and ^{99m}Tc-tetrofosmin in the field of nuclear cardiology, the two ^{99m}Tc-based monocationic complexes

still have the drawbacks, such as low first-pass myocardial extraction, underestimation of the myocardial blood flow at high flow rates, and relatively high liver uptake.[16,17] With the development of myocardial molecular imaging probes, radionuclide-labeled $TPPs^+$ derivatives for mitochondria targeting have become the focus of research.[14,15,18,19] Compared with ^{99m}Tc, the chemistry of iodine is well defined and more suited for labeling the small molecules with biological activity. Four radioiodine isotopes are commonly used in nuclear medicine. ^{123}I (*EC*, $E_\gamma = 159$ keV, $T_{1/2} = 13.2$ h) is used for single photon emission computed tomography (SPECT). ^{124}I (EC/β^+, $T_{1/2} = 4.18$ d) is currently applied in positron emission tomography (PET). ^{131}I (β^-, $T_{1/2} = 8.04$ d) therapy is an effective measure for the radiation treatment. ^{125}I (*EC*, $E_\gamma = 35$ keV, $T_{1/2} = 59.4$ d) is particularly well suited for kinds of researches such as receptor binding assays and biodistribution studies. However, to date, only a handful of radioiodine-labeled $TPPs^+$ methods have been reported. Typical examples include (1) the radiosynthesis of ^{125}I-labeled $TPPs^+$ that is based on trans-vinylboronic acid reported by Srivastava's group[18] and (2) a two-step method using the tributylstannyl as the labeling precursors reported by Yasuhiro Magata's group.[19] These methods mentioned above still hold the drawbacks of multi-step reactions, long reaction time, and low radiochemical yield, which hinder their further application. In order to provide clinicians more choices, we developed an efficient one-step method to obtain radioiodine-labeled $TPPs^+$ using corresponding phenylboronic-TPP as labeling precursors (Scheme 1). In theory, the method of radiolabeling has commonalities between the four radioiodine nuclides. With the establishment of this new synthetic approach, we prepared a series of *meta*-^{125}I-labeled $TPPs^+$ with or without methoxy group, and evaluated the potential application of these compounds as mitochondria targeting probes.

2 | EXPERIMENTAL

2.1 | General

All reagents used for chemistry and biology were purchased from commercial sources and used without further purification. [^{125}I]NaI was purchased from PerkinElmer. Reactions were controlled by thin layer chromatography on aluminum TLC plates, silica gel 60 coated with fluorescent indicator F254

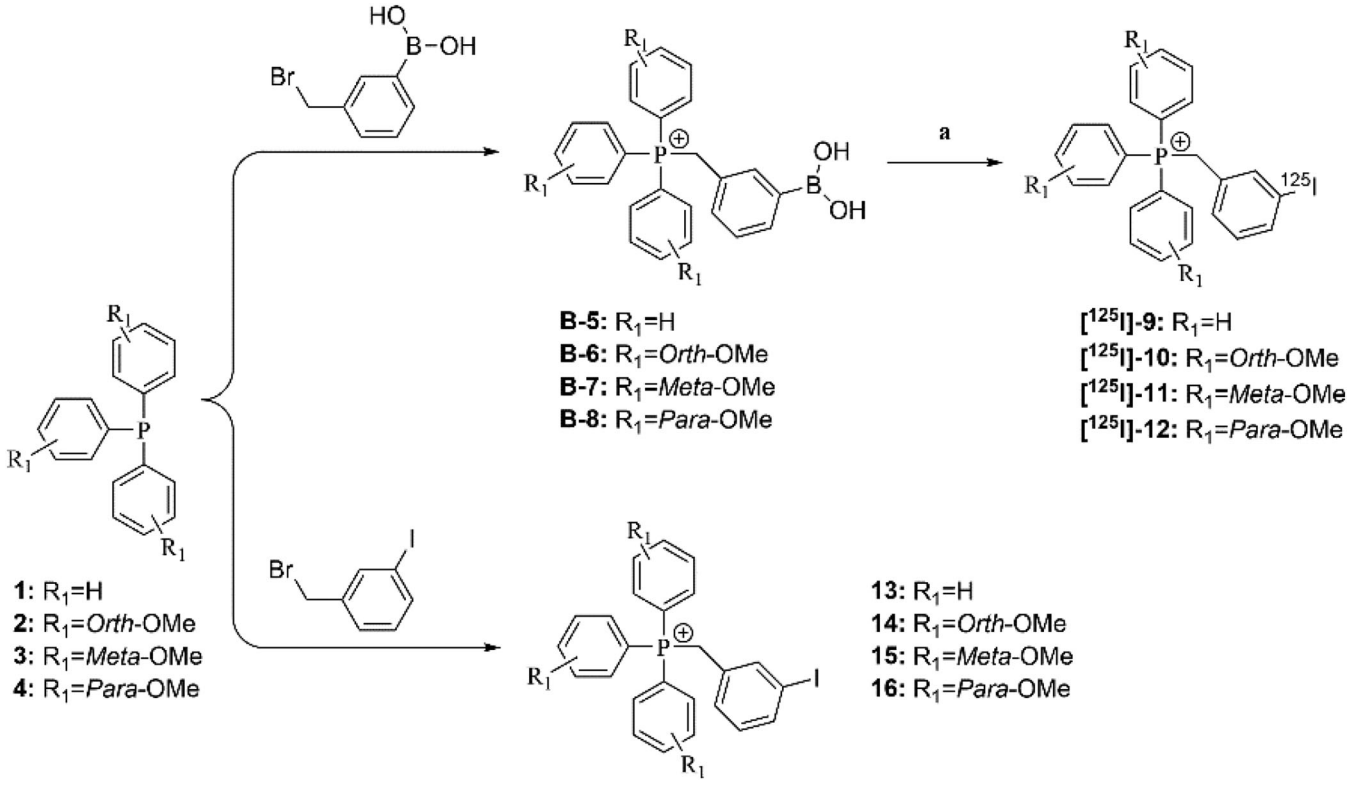

SCHEME 1 Synthetic route of benzyl TPP cations **[^{125}I] 9–[^{125}I] 12** and the corresponding nonradioactive reference compounds **13–16**. a. [^{125}I]NaI, Cu_2O, 1,10-phenamthroline, rt, 1 h

(Merck, German), and visualized under ultraviolet light (254 nm). ^{1}H and ^{13}C NMR spectra were detected by a JEOL JNM-ECZ (600 MHz) spectrometer and a Bruker (400 MHz) spectrometer. ^{31}P NMR spectra were detected on a Bruker (400 MHz) spectrometer. High-resolution mass spectra (HRMS) were obtained by a Bruker microTOF-QII or AB SCIEX Triple TOF™ 5600^{+} mass spectrometer. High-performance liquid chromatography (HPLC) was achieved on a Shimadzu SCL-20 AVP HPLC system equipped with a SPD-M20AUV-Vis detector and a Bioscan Flow Count 3200 NaI/PMT γ-radiation scintillation detector. The HPLC methods were shown as following: A: water; B: 0.1% trifluoroacetic acid in acetonitrile, 0–2.0 min, 10% B; 2.0–15.0 min, 10%–90% B; 15.0–20.0 min, 90%–10% B, flow rate: 1 ml/min for analytical column (Kromasil 100-5-C18, 250 × 4.6 mm).

The rat embryonic cardiomyoblast cell line (H9c2) and mouse normal fibroblast cell line (NIH/3T3) were obtained from China Infrastructure of Cell Line Resources and cultured in DMEM medium containing 10% fetal bovine serum (Gibco) and 1% penicillin-streptomycin. Cell lines were all incubated as a monolayer at 37°C with saturated humidity and 5% CO_2.

Radioactive count was measured on a PerkinElmer Automatic Gamma Counter system (WIZARD2, 2480). The Kunming mice (18–22 g, female) were purchased from Beijing Vital River Laboratories. All protocols related to the use of animals were approved by the Institutional Animal Care Committee of Beijing Normal University.

2.2 | Synthesis procedure and characterization

2.2.1 | (3-Boronobenzyl) triphenylphosphonium cation (B-5)

A mixture of triphenylphosphine (0.472 g, 1.8 mmol) and (3-(bromomethyl)phenyl)boronic acid (0.279 g, 1.3 mmol) in 4 ml of toluene was heated at 60°C for 3 h. Then, toluene was removed by vacuum. The crude product was purified via column chromatography (silica gel, 20:1 [v/v] dichloromethane/methanol) to obtain **B-5** as a white solid (0.386 g, 74.8%). ^{1}H NMR (600 MHz, MeOD-d_4, chemical shift δ in ppm relative to TMS): δ 7.89–7.85 (m, 3H), 7.71–7.67 (m, 6H), 7.65–7.59 (m, 6H), 7.43 (d, $J = 7.6$ Hz, 2H,), 6.96 (m, 2H), 4.89 (d, $J = 15.1$ Hz, 2H). ^{13}C NMR (150 MHz, MeOD-d_4): δ 135.15, 135.13, 134.07, 134.00, 133.79, 130.06, 129.97, 118.10, 117.53, 29.56. ^{31}P NMR (400 MHz, MeOD-d_4): δ 23.3978. HRMS (+TOF MS): m/z calculated for $C_{25}H_{23}BO_2P^{+}$ $[M]^{+}$ 397.1523, found 397.1367.

2.2.2 | (3-Boronobenzyl)-tris (2-methoxyphenyl)phosphonium cation (B-6)

B-6 (white solid, 0.498 g, 78.7%) was prepared as the same way described above. ^{1}H NMR (600 MHz, MeOD-d_4, chemical shift δ in ppm relative to TMS): δ 7.75 (t, $J = 7.9$ Hz, 3H), 7.46–7.30 (m, 5H), 7.21–7.16 (m, 6H,), 7.12 (s, 2H), 4.70 (s, 2H), 3.63 (s, 9H). ^{13}C NMR (101 MHz, MeOD-d_4): δ 161.62 (d, $J_{cp} = 2.4$ Hz), 136.78 (d, $J_{cp} = 2.2$ Hz), 135.74, 135.07 (d, $J_{cp} = 8.2$ Hz), 133.81 (d, $J_{cp} = 3.7$ Hz), 132.71, 132.48, 131.29, 127.42, 121.51 (d, $J_{cp} = 12.8$ Hz), 112.47 (d, $J_{cp} = 6.8$ Hz), 106.18 (d, $J_{cp} = 91.8$ Hz), 55.15, 30.18 (d, $J_{cp} = 53.0$ Hz). ^{31}P NMR (400 MHz, MeOD-d_4): δ 25.1112. HRMS (+TOF MS): m/z calculated for $C_{28}H_{29}BO_5P^{+}$ $[M]^{+}$ 487.1840, found 487.1850.

2.2.3 | (3-Boronobenzyl)-tris (3-methoxyphenyl)phosphonium cation (B-7)

B-7 (white solid, 0.523 g, 82.6%) was prepared as the same way described above. ^{1}H NMR (600 MHz, MeOD-d_4, chemical shift δ in ppm relative to TMS): δ 7.61 (td, $J = 8.0$, 4.5 Hz, 4H), 7.42 (d, $J = 8.5$ Hz, 3H), 7.29 (s, 1H), 7.25 (t, $J = 7.5$ Hz, 1H), 7.15 (dd, $J = 12.5$, 7.7 Hz, 3H), 7.08 (dd, $J = 13.8$, 1.7 Hz, 4H), 4.91 (d, $J = 14.8$ Hz, 2H), 3.76 (s, 9H). ^{13}C NMR (101 MHz, MeOD-d_4): δ 160.61 (dd, $J_{cp} = 15.9$, 0.9 Hz), 133.76, 133.73 (d, $J_{cp} = 0.9$ Hz), 132.15, 131.44 (d, $J_{cp} = 15.2$ Hz), 128.19, 126.11 (d, $J_{cp} = 9.5$ Hz), 120.83, 119.39, 118.89 (d, $J_{cp} = 10.2$ Hz), 118.54, 55.07, 29.48 (d, $J_{cp} = 47$ Hz). ^{31}P NMR (400 MHz, MeOD-d_4): δ 23.9460. HRMS (+TOF MS): m/z calculated for $C_{28}H_{29}BO_5P^{+}$ $[M]^{+}$ 487.1840, found 487.1846.

2.2.4 | (3-Boronobenzyl)-tris (4-methoxyphenyl)phosphonium cation (B-8)

B-8 (white solid, 0.563 g, 88.9%) was prepared as the same way described above. ^{1}H NMR (600 MHz, MeOD-d_4, chemical shift δ in ppm relative to TMS): δ 7.66 (s, 1H), 7.48 (m, 6H), 7.19–7.17 (m, 8H), 7.05 (d, $J = 7.2$ Hz, 1H), 4.66 (s, 2H), 3.90 (s, 9H). ^{13}C NMR (150 MHz, MeOD-d_4): δ 166.41 (d, $J_{cp} = 2.6$ Hz), 137.99, 137.33 (d, $J_{cp} = 7.4$ Hz), 134.81, 133.74, 133.47, 129.26 (d, $J_{cp} = 17.1$ Hz), 128.58 (d, $J_{cp} = 27.1$ Hz), 116.94 (d, $J_{cp} = 25.8$ Hz), 109.58 (d, $J_{cp} = 13.7$ Hz), 55.21, 31.07 (d, $J_{cp} = 60.6$ Hz). ^{31}P NMR (400 MHz, MeOD-d_4): δ 21.4810. HRMS (+TOF MS): m/z calculated for $C_{28}H_{29}BO_5P^{+}$ $[M]^{+}$ 487.1840, found 487.1846.

2.2.5 | (3-Iodobenzyl)-trisphenylphosphonium (13)

A mixture of triphenylphosphine (0.340 g, 1.3 mmol) and 3-iodobenzyl bromide (0.504 g, 1.7 mmol) in 4 ml of toluene was heated at 60°C for 7 h. After cooling to ambient temperature, the solvents were removed by evaporation under vacuum, and the obtained residue was washed with diethyl ether for twice, dried, and directly obtained **13** as a white solid (0.601 g, 96.6%). ^{1}H NMR (600 MHz, MeOD-d_4, chemical shift δ in ppm relative to TMS): δ 7.91–7.87 (td, $J = 7.4$, 1.3 Hz, 3H), 7.69–7.73 (m, 6H), 7.67–7.61 (m, 7H), 7.22 (dd, $J = 3.9$, 1.8 Hz, 1H), 7.03 (d, $J = 7.7$ Hz, 1H), 6.99 (t, $J = 7.8$ Hz, 1H), 4.85 (d, $J = 15.1$ Hz, 2H). ^{31}P NMR (400 MHz, MeOD-d_4): δ 23.7438. HRMS (+TOF MS): m/z calculated for $C_{25}H_{21}IP^+$ $[M]^+$ 479.0420, found 479.0417.

2.2.6 | (3-Iodobenzyl)-tris(2-methoxyphenyl) phosphonium (14)

14 (white solid, 0.704 g, 95.2%) was prepared as the same way described above. ^{1}H NMR (600 MHz, MeOD-d_4, chemical shift δ in ppm relative to TMS): δ 7.79–7.75 (m, 3H), 7.49–7.45 (m, 2H), 7.44–7.40 (m, 3H), 7.23–7.17 (m, 7H), 6.89 (t, $J = 8.1$ Hz, 1H), 4.67 (d, $J = 16.1$ Hz, 2H), 3.64 (s, 9H). ^{31}P NMR (400 MHz, MeOD-d_4): δ 25.4596. HRMS (+TOF MS): m/z calculated for $C_{28}H_{27}IO_3P^+$ $[M]^+$ 569.0737, found 569.0735.

2.2.7 | (3-Iodobenzyl)-tris(3-methoxyphenyl) phosphonium (15)

15 (white solid, 0.694 g, 93.8%) was prepared as the same way described above ^{1}H NMR (600 MHz, MeOD-d_4, chemical shift δ in ppm relative to TMS): δ 7.68 (d, $J = 7.8$ Hz, 1H), 7.65–7.62 (m, 3H), 7.44 (d, $J = 9.4$ Hz, 3H), 7.30 (s, 1H), 7.19–7.16 (m, 3H), 7.10 (d, $J = 13.9$ Hz, 4H), 7.02 (t, $J = 7.8$ Hz, 1H), 4.88 (s, 2H), 3.80 (s, 9H). ^{31}P NMR (400 MHz, MeOD-d_4): δ 24.2542. HRMS (+TOF MS): m/z calculated for $C_{28}H_{27}IO_3P^+$ $[M]^+$ 569.0737, found 569.0739.

2.2.8 | (3-Iodobenzyl)-tris(4-methoxyphenyl) phosphonium (16)

16 (white solid, 0.712 g, 96.2%) was prepared as the same way described above ^{1}H NMR (600 MHz, MeOD-d_4, chemical shift δ in ppm relative to TMS): δ 7.65 (d, $J = 7.7$ Hz, 1H), 7.50–7.47 (m, 6H), 7.22–7.10 (m, 6H), 7.18 (d, $J = 2.3$ Hz, 1H), 7.04 (d, $J = 8.0$ Hz, 1H), 7.00 (t, $J = 7.8$ Hz, 1H), 4.62 (d, $J = 17.9$ Hz, 2H). 3.91 (s, 9H). ^{31}P NMR (400 MHz, MeOD-d_4): δ 21.7485. HRMS (+TOF MS): m/z calculated for $C_{28}H_{27}IO_3P^+$ $[M]^+$ 569.0737, found 569.0735.

2.3 | Radiochemistry

The *meta*-^{125}I-TPPs$^+$, **[^{125}I] 9–[^{125}I] 12** were synthesized from the corresponding phenylboronic acid labeling precursors via an optimized copper-catalyzed method **(shown** in Scheme 1).[20] Briefly, a freshly prepared mixture of Cu_2O (4 μmol), 1,10-phenanthroline (8 μmol) in 0.8 ml of acetonitrile and 0.2 ml of water was stirred for 10 min at room temperature. In a reaction vial, the corresponding phenylboronic precursor (0.5 mg, 1 μmol) was dissolved in 100 μl of acetonitrile followed by the addition of 100 μl of Cu_2O/1,10-phenanthroline mixture and ^{125}I-NaI (14.8 MBq, 4–5 μl). The vial was not sealed to allow air entering through a simple activated carbon adsorption unit and kept at room temperature for another 60 min. The final products were purified by HPLC, and their radiochemical purities and specific activities were also determined.

2.4 | Stability study

In stability experiment, the purified ^{125}I-TPPs$^+$, **[^{125}I] 9–[^{125}I] 12**, were added to physiological saline (0.9%) and incubated at room temperature for 6 h, respectively. Samples of the resulting solutions were analyzed by radio-HPLC.

In vitro serum stability experiment, 50 μl of the ^{125}I-TPPs$^+$ (**[^{125}I]-9**, **[^{125}I]-10**, **[^{125}I]-11**, or **[^{125}I]-12**) solution was added to 0.1 ml of mouse serum and incubated at 37°C for 2 h, respectively. Then 500 μl of acetonitrile was added to precipitate the serum proteins. After centrifugation for 5 min, the supernatants were filtered through a 0.2-μm Millipore filter and analyzed by radio-HPLC.

2.5 | Determination of the octanol–water partition coefficient (log *P*)

The log *P* values of ^{125}I-labeled TPPs$^+$ were determined by measuring the distribution of the radiotracer between octanol (organic phase) and phosphate-buffered saline (PBS, 0.05 mol/L, pH = 7.4, aqueous phase). Firstly, mixing 20 μl of the purified radiotracers solution with 480 μl of PBS and 500 μl of *n*-octanol in a 2.0-ml EP microtube. After vigorously vortexing for 3 min, the tube

was centrifugated for 5 min at 10,000 rpm. The radioactive counts in 100-μl aliquots of both phases were measured by a gamma counter. The octanol-water partition coefficient (log *P*) was calculated using the following equation: $P =$ (activity in octanol-background activity)/(activity in aqueous layer-background activity). The log *P* value was reported as mean ± standard deviation (SD) of triplicate samples.

2.6 | In vitro cellular uptake assay

The cellular uptake studies of ^{125}I-labeled TPPs$^+$ were performed in the rat embryonic cardiomyoblast cell line (H9c2) and mouse normal fibroblast cell line (NIH/3T3). Cells were seeded in 24-well plates at a density of 2×10^5 cells/well and cultured for 24 h at 37°C under saturated humidity and 5% CO_2. To further evaluate the mitochondrial membrane potential, the H9c2 cells were allowed to pretreat with carbonyl cyanide *m*-chlorophenylhydrazone (CCCP, 10 μM in 50-mM low-K$^+$ HEPES buffer) for 30 min prior to the experiment. The adherent cells were washed twice with 1-ml culture medium, followed by addition of ^{125}I-labeled TPPs$^+$ (11.7 KBq in 600 μl of DMED medium per well). After incubation at 37°C for 30 min, the medium was removed, and the cells were washed with ice-cold PBS (0.01 mol/L, pH = 7.4, containing 0.2% BSA) and lysed with 0.5-ml NaOH (1 mol/L), respectively. The lysate was analyzed by γ-counter. All assays were studied in triplicate and repeated three times.

2.7 | Biodistribution studies

All biodistribution studies were performed under a protocol approved by the Beijing Administration Office of Laboratory Animal (BAOLA). The ex vivo biodistribution studies were performed on Kunming mice (female, 4–5 weeks of age, 18–2 g, $n = 4$). The HPLC-purified ^{125}I-TPPs$^+$ (**[^{125}I]-9**, **[^{125}I]-10**, **[^{125}I]-11**, or **[^{125}I]-12**, 37 KBq diluted in 0.1 ml of saline) was administered into the mice via the tail vein. At the selected time point, (5, 30, 60, or 120 min), the mice were sacrificed. The tissues and organs of interest were collected, weighed, and counted by a γ-counter. The percentage of injected dose per gram (%ID/g) for each sample was calculated and expressed as mean ± SD.

2.8 | Statistical methods

Statistical analysis was performed using the unpaired t-test with commercial software (GraphPad Prism 8.0 Software™, La Jolla, CA, USA). Difference at the 95% confidence level ($p < 0.05$) was considered to be statistically significant.

3 | RESULTS AND DISCUSSION

3.1 | Chemistry and radiochemistry

The synthetic routes of the *meta*-^{125}I-labeled-TPPs$^+$ and the corresponding nonradioactive reference com-pounds were shown in Scheme 1. The four radiolabeling precursors, **B-5**, **B-6**, **B-7**, and **B-8**, were obtained by coupling the (3-(bromomethyl)phenyl)boronic acid with **1** or the *ortho/meta/para*-methoxy groups modified TPPs, **2, 3**, and **4**, respectively. The aimed compounds were characterized by ^{1}H NMR, ^{13}C NMR, ^{31}P NMR, and HRMS. The purities of all the above compounds were greater than 95%, as determined by HPLC (shown in Table 1).

The nonradioactive compounds **(13–16)**, commonly used as structure-referenced congeners of *meta*-^{125}I-labeled-TPPs$^+$, were obtained by coupling 1-(bromomethyl)-3-iodobenzene with **1, 2, 3**, and **4**, respectively. The targeted compounds were characterized by NMR (^{1}H, ^{31}P) and HRMS.

The labeling efficiency and radiochemical purity of *meta*-^{125}I-labeled-TPPs$^+$ were determined by Radio-HPLC. The HPLC retention time of ^{125}I$^-$ was found to be 3.24 min, while those of **[^{125}I] 9–[^{125}I] 12** were 16.11, 16.20, 16.29, and 16.08 min, respectively, which agreed with the retention time of non-radioactive compounds (As shown in Table 1 and Figure 1).

The *meta*-^{125}I-labeled-TPPs$^+$ were synthesized based on a simple one-step copper-mediated radioiodination method (Scheme 1). In order to optimize the reaction conditions, the effects of the solvents, Cu_2O/1, 10-phenanthroline concentrations and reaction temperature on the radiochemical yield of **[^{125}I]-9** were investigated. The best solvent condition of Cu_2O/1, 10-phenanthroline mediated radioiodination reported in literature was acetonitrile.[21] However, lower radiochemical yield of **[^{125}I]-9** (<50%) was observed when acetonitrile was used alone. The labeling efficiency could be significantly improved by adding an aliquot of water. The yield of the reaction decreased (<70%) when the reaction temperature raised to 100°C. In addition, a very inferior radiochemical yield (<10%) was also found when the reaction vial was sealed, which indicated that oxygen might be required in the labeling process. It has been reported that an oxidative process was involved in the formation of iodobenzene intermediate during the copper-catalyst Chan–Evans–Lam cross-coupling reaction.[22] In this copper-catalyst radioiodination reaction, oxygen in air

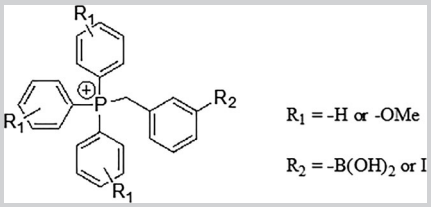

TABLE 1 The chemical or radiochemical yields, the HPLC retention times and log *P* values of compounds

Entry	Compound	R_1	R_2	Yield[a]	HPLC R_t/min	Log *P*
1	**B-5**	H	$B(OH)_2$	74.8%	14.55	-
2	**B-6**	*o-OMe*	$B(OH)_2$	78.7%	14.52	-
3	**B-7**	*m-OMe*	$B(OH)_2$	82.6%	14.74	-
4	**B-8**	*p-OMe*	$B(OH)_2$	88.9%	14.38	-
5	**[^{125}I]-9**	H	^{125}I	>95%	16.11	1.26 ± 0.03
6	**[^{125}I]-10**	*o-OMe*	^{125}I	>95%	16.20	1.47 ± 0.04
7	**[^{125}I]-11**	*m-OMe*	^{125}I	>95%	16.29	1.59 ± 0.06
8	**[^{125}I]-12**	*p-OMe*	^{125}I	>95%	16.08	1.31 ± 0.03
9	**13**	H	^{127}I	96.6%	15.59	-
10	**14**	*o-OMe*	^{127}I	95.2%	15.68	-
11	**15**	*m-OMe*	^{127}I	93.8%	15.73	-
12	**16**	*p-OMe*	^{127}I	96.2%	15.41	-

[a]Yields shown are chemical or radiochemical yield.

may play an important role as the oxidant. Thus, the optimal labeling conditions of **[^{125}I]-9** were as follows: 1 μmol of phenylboronic precursor, Cu_2O/1,10-phenanthroline (0.4 μmol/0.8 μmol) in 0.2 ml of acetonitrile/water (9:1, v/v) mixture solvent, 5 μl of [^{125}I]NaI, incubating in air atmosphere at room temperature for 60 min.

Under these optimized conditions, radioiodinations of the *OMe*-modified triphenylphosphine-phenylboronic acids, **B 6–B 8**, were also investigated, and the corresponding aim products, **[^{125}I] 10–[^{125}I] 12** were obtained in high radiochemical yields (>95%). The result suggested that the *OMe*-substituents in the triphenylphosphine-phenylboronic acids did not obviously affect the efficiency of the reactions. The ^{125}I-TPPs$^+$ could sufficiently separate from the excess labeling precursors with further HPLC purification and obtained the final products with high specific activity (>46.6 GBq/μmol). The labeling results suggested that the present procedure is a simple, condition mildly, and efficient copper-catalyzed method for the synthesis of ^{125}I-labeled TPPs$^+$ derivatives.

The log *P* of **[^{125}I] 9–[^{125}I] 12** in octanol and PBS (0.05 mol/L, pH = 7.4) were 1.26 ± 0.03, 1.47 ± 0.04, 1.59 ± 0.06, and 1.31 ± 0.03, respectively. All of these ^{125}I-TPPs$^+$ remain stable in saline at room temperature for 6 h, and only intact ^{125}I-TPPs$^+$ were detected by RP-HPLC. After 2 h of incubation in mouse serum, the radiochemical purity of ^{125}I-TPPs$^+$ remained in the range of 90–95%. Only the *ortho*-methoxy group modified compound, **[^{125}I]-10**, displayed slight deiodination in mouse serum at 37°C for 2 h (Figure 1).

3.2 | In vitro cellular uptake studies

In vitro cellular uptake experiments of the ^{125}I-TPPs$^+$, **[^{125}I] 9-[^{125}I] 12** were performed on H9c2 cells, a rat embryonic cardiomyoblast cell line with overexpressed mitochondria, and NIH/3T3 cells, a mouse normal fibroblast cell line as a negative control. CCCP is reported to be a chemical inhibitor of oxidative phosphorylation that can depolarize the mitochondria membrane potential. To further confirm whether the radiotracer **[^{125}I] 9–[^{125}I] 12** localized in the cells through mitochondrial membrane potential, the cellular uptakes on CCCP pretreated H9c2 cells were also studied.

As shown in Figure 2, in H9c2 cell line, **[^{125}I] 9–[^{125}I] 12** displayed a relatively high cellular uptake of 7.1% ± 0.4%, 7.7% ± 1.2%, 7.6% ± 0.4%, and 9.1% ± 0.6% of the total added radioactivity, respectively. However, the radioactivity accumulation of **[^{125}I] 9–[^{125}I] 12** in NIH/3T3 was only 56%, 51%, 50%, and 41% of those in H9c2 cell line, respectively. After the CCCP pretreatment,

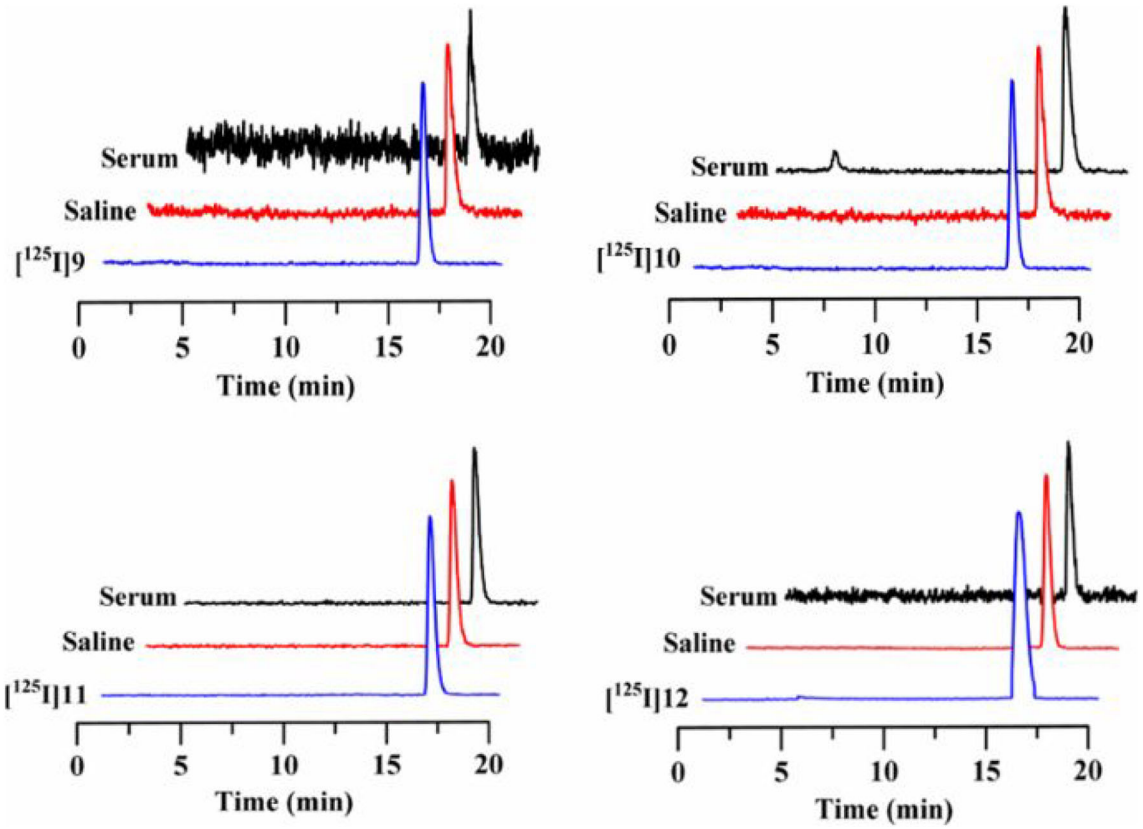

FIGURE 1 The radio-HPLC chromatograms of the ^{125}I-labeled TPPs^{+} before and after incubating at room temperature in saline for 6 h and at 37°C in the mice serum for 2 h. The retention times of **[^{125}I] 9–[^{125}I] 12** were 16.11, 16.20, 16.29, and 16.08 min, respectively

FIGURE 2 Cellular uptakes of the ^{125}I-labeled TPPs^{+} in H9c2 (with or without CCCP) and NIH/3T3 cells at 37°C for 30 min. *$p < 0.05$ shows significant differences between groups

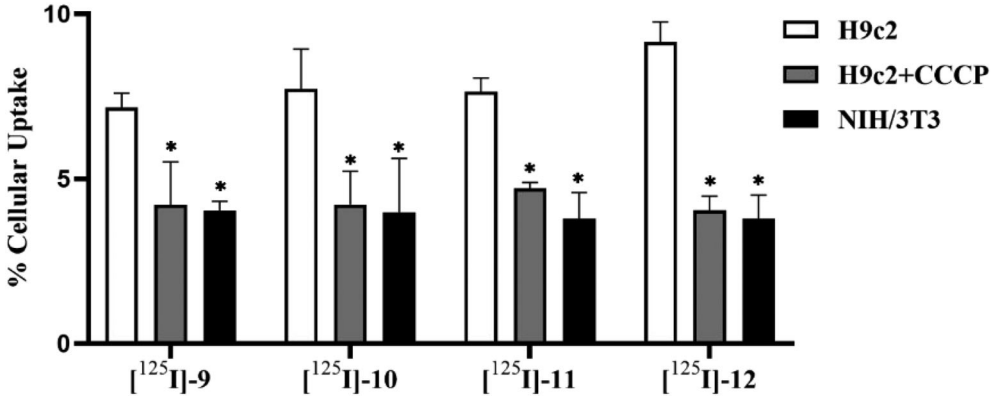

the cellular uptakes of **[^{125}I] 9–[^{125}I] 12** in H9c2 cell line decreased to 58%, 55%, 62%, and 45%, respectively ($p < 0.05$). It demonstrated that these ^{125}I-TPPs^{+} accumulated in the cardiomyoblast cells through the specific mitochondrial membrane potential pathway.

3.3 | Ex vivo biodistribution study

The ex vivo biodistribution studies of ^{125}I-TPPs^{+} were performed on Kunming mice to investigate the pharmacokinetic properties. The results of the biodistribution studies are shown in Tables 2–5.

[^{125}I]-9 displayed a moderate initial accumulation in heart (6.31 ± 0.59%ID/g at 5 min p.i.) and good retention (5.44 ± 0.25% ID/g at 120 min p.i.). The uptake in lung and blood at 5 min p.i. was 4.13 ± 0.56%ID/g and 1.34 ± 0.16%ID/g, respectively. The heart/lung and heart/blood ratios were 2.78 and 28.63 at 120 min p.i., respectively. The radioactivity accumulations of [^{125}I]-9 in the liver, intestine, and kidneys were remarkably high, which indicated the radioactivity of [^{125}I]-9 might be

TABLE 2 Biodistribution data of **[^{125}I]-9** in female Kunming mice ($n = 4$, mean ± SD, %ID/g)

Organ	Uptake			
	5 min	30 min	60 min	120 min
Heart	6.31 ± 0.59	5.81 ± 0.44	5.54 ± 0.08	5.44 ± 0.25
Liver	34.85 ± 3.26	31.79 ± 2.71	20.53 ± 2.26	12.30 ± 1.48
Lung	4.13 ± 0.56	2.85 ± 0.38	2.73 ± 0.44	1.96 ± 0.16
Kidneys	80.07 ± 1.00	76.82 ± 1.85	77.13 ± 2.37	64.23 ± 3.10
Spleen	5.11 ± 1.69	3.42 ± 0.42	3.85 ± 0.61	3.28 ± 0.27
Stomach	2.44 ± 0.65	3.21 ± 0.13	5.31 ± 1.11	4.99 ± 0.30
Bone	1.79 ± 0.33	2.17 ± 0.08	2.15 ± 0.44	1.49 ± 0.15
Muscle	1.76 ± 0.16	1.61 ± 0.21	1.77 ± 0.17	1.72 ± 0.12
Intestine	4.29 ± 0.67	4.96 ± 0.30	17.86 ± 0.80	19.92 ± 1.47
Blood	1.34 ± 0.16	1.07 ± 0.15	0.36 ± 0.02	0.19 ± 0.00
Thyroid (%ID)	0.13 ± 0.04	0.43 ± 0.04	0.62 ± 0.12	0.47 ± 0.04

TABLE 3 Biodistribution data of **[^{125}I]-10** in female Kunming mice ($n = 4$, mean ± SD, %ID/g)

Organ	Uptake			
	5 min	30 min	60 min	120 min
Heart	7.76 ± 0.50	5.70 ± 0.28	5.69 ± 0.33	4.49 ± 0.19
Liver	47.18 ± 3.50	11.17 ± 0.35	6.64 ± 0.26	4.31 ± 0.24
Lung	11.26 ± 3.44	5.50 ± 1.22	4.75 ± 0.25	1.59 ± 0.04
Kidneys	77.90 ± 2.38	80.56 ± 1.12	58.46 ± 2.17	35.64 ± 1.18
Spleen	19.42 ± 3.04	8.69 ± 0.22	5.64 ± 0.98	3.66 ± 0.40
Stomach	2.96 ± 0.20	6.35 ± 0.62	5.72 ± 1.16	5.00 ± 0.68
Bone	4.57 ± 0.55	3.68 ± 0.30	3.49 ± 0.22	2.67 ± 0.18
Muscle	2.03 ± 0.49	2.41 ± 0.44	2.24 ± 0.17	1.02 ± 0.31
Intestine	6.40 ± 0.40	28.32 ± 2.41	16.68 ± 0.97	5.88 ± 0.93
Blood	3.68 ± 0.53	1.07 ± 0.15	0.65 ± 0.06	0.34 ± 0.05
Thyroid (%ID)	0.16 ± 0.07	0.19 ± 0.09	1.01 ± 0.02	0.92 ± 0.01

TABLE 4 Biodistribution data of **[^{125}I]-11** in female Kunming mice ($n = 4$, mean ± SD, %ID/g)

Organ	Uptake			
	5 min	30 min	60 min	120 min
Heart	6.01 ± 0.51	5.14 ± 0.29	4.98 ± 0.36	4.50 ± 0.36
Liver	86.47 ± 2.15	31.49 ± 1.95	22.31 ± 1.64	14.75 ± 1.67
Lung	8.51 ± 0.22	5.30 ± 0.48	4.17 ± 0.57	2.35 ± 0.14
Kidneys	81.44 ± 1.88	56.51 ± 2.14	46.20 ± 2.49	35.02 ± 1.54
Spleen	12.78 ± 0.92	11.00 ± 0.53	8.46 ± 0.56	6.22 ± 0.44
Stomach	4.82 ± 0.36	10.08 ± 0.52	10.47 ± 1.20	9.69 ± 0.92
Bone	3.66 ± 0.32	3.17 ± 0.52	3.23 ± 0.23	2.59 ± 0.56
Muscle	1.21 ± 0.16	1.49 ± 0.13	1.46 ± 0.23	1.08 ± 0.13
Intestine	10.89 ± 1.29	79.19 ± 0.80	29.60 ± 2.14	17.44 ± 1.04
Blood	3.19 ± 0.24	1.54 ± 0.24	0.92 ± 0.09	0.51 ± 0.02
Thyroid (%ID)	0.17 ± 0.06	0.46 ± 0.10	0.51 ± 0.13	0.66 ± 0.38

TABLE 5 Biodistribution data of **[^{125}I]-12** in female Kunming mice ($n = 4$, mean ± SD, %ID/g)

Organ	Uptake			
	5 min	30 min	60 min	120 min
Heart	2.70 ± 0.15	2.43 ± 0.30	2.38 ± 0.18	2.36 ± 0.25
Liver	24.55 ± 1.78	9.86 ± 1.16	5.84 ± 0.82	5.79 ± 0.30
Lung	5.16 ± 0.62	2.76 ± 0.24	1.37 ± 0.43	1.19 ± 0.32
Kidneys	32.12 ± 1.00	30.31 ± 1.35	19.47 ± 0.78	19.31 ± 0.26
Spleen	7.94 ± 0.65	6.02 ± 1.29	3.15 ± 0.89	2.57 ± 0.14
Stomach	2.00 ± 0.91	2.61 ± 0.50	2.89 ± 1.54	3.94 ± 0.38
Bone	1.71 ± 0.35	1.47 ± 0.09	1.39 ± 0.20	1.35 ± 0.37
Muscle	0.65 ± 0.13	0.62 ± 0.20	0.64 ± 0.12	0.74 ± 0.03
Intestine	8.50 ± 1.78	11.72 ± 2.01	8.89 ± 1.57	8.18 ± 1.45
Blood	1.45 ± 0.15	0.49 ± 0.21	0.12 ± 0.10	0.08 ± 0.04
Thyroid (%ID)	0.32 ± 0.47	0.21 ± 0.10	0.20 ± 0.08	0.20 ± 0.18

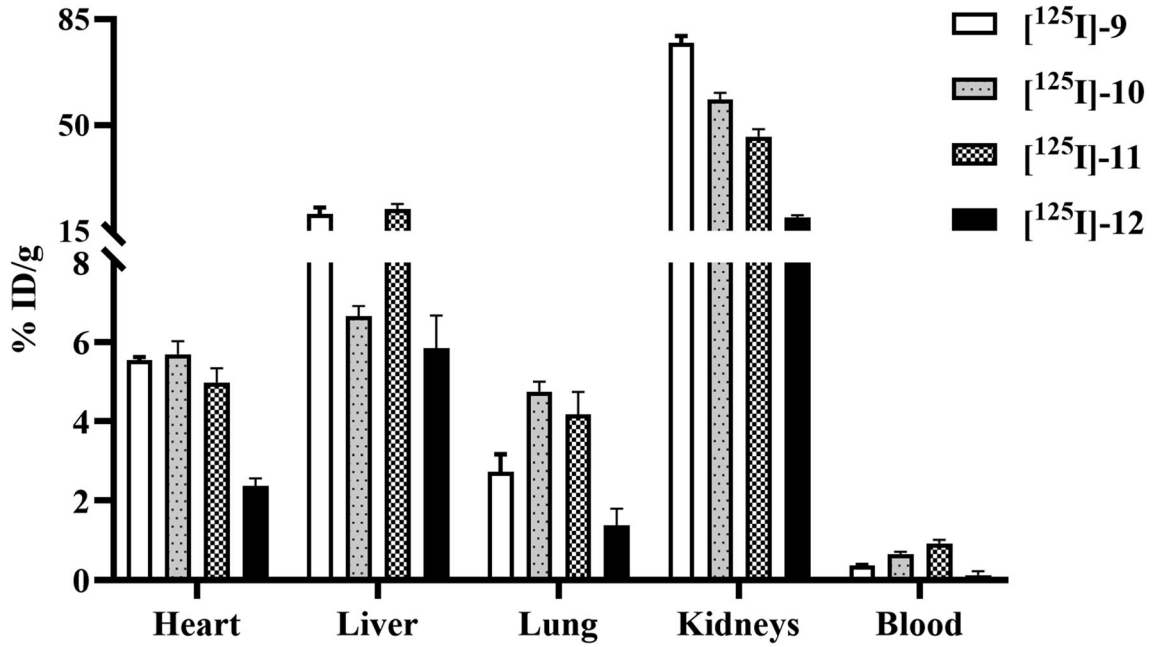

FIGURE 3 Comparison of organ uptake (heart, liver, lung, kidneys, and blood) between **[^{125}I] 9** and **[^{125}I] 12** in Kunming mice (%ID/g, 60 min post-injection, $n = 4$)

excreted from the body via both the hepatobiliary and renal systems. Actually, for the mitochondrial membrane potential based imaging agent, the high liver uptake is a drawback, which will interfere with the imaging quality of myocardium (low signal-to-noise ratio), as well as tracing tumors in chest and abdomen.

In many cases, the methoxy group introduced in TPPs$^+$ radiotracers could act as a positive effect on their pharmacokinetic properties by accelerating the radioactivity clearance from liver and other non-targeting organs.[22,23] In this study, three methoxy group introduced ^{125}I-TPPs$^+$, **[^{125}I]-10**, **[^{125}I]-11**, and **[^{125}I]-12** were designed and synthesized based on the architecture of **[^{125}I]-9**. The methoxy groups were introduced into the phenyl groups of triphenylphosphine moieties on *para*, *ortho*, and *meta* positions, respectively. As expected, the liver clearance of three methoxy group modified ^{125}I-TPPs$^+$ was significantly quicker than that of **[^{125}I]-9**. At 60 min post-injection, the liver uptakes of **[^{125}I]-10**, **[^{125}I]-11**, and **[^{125}I]-12** were rapidly decreased to 14.1%, 25.8%, and 23.8% from the maximum values, respectively. And the liver accumulation of **[^{125}I]-9** still remained 58.9% of the maximum uptakes at 60 min post-injection. Moreover, focusing on the uptake of 60 min post-injection (Figure 3), it was found that not only the introduction of methoxy groups, but also the position of

methoxy groups of ^{125}I-TPPs^{+} functioned a significant effect on their pharmacokinetic properties. The *meta-OMe* modified [**^{125}I]-11** displayed a higher liver uptake (22.31 ± 1.64%ID/g), while [**^{125}I]-10** and [**^{125}I]-12** contained methoxy groups on the *ortho* and *para* positions, respectively, displayed a decreased liver uptake (6.64 ± 0.26 and 5.84 ± 0.82%ID/g, respectively) than those of [**^{125}I]-11** and [**^{125}I]-9** (20.53 ± 2.26%ID/g). The *para-OMe* modified ^{125}I-TPPs^{+}, [**^{125}I]-12** also displayed a significant lower radioactivity accumulation in heart, lungs and blood than those of other ^{125}I-TPPs^{+}.

Compared with the [**^{125}I]-9**, the lipophilicity of [**^{125}I] 10–[^{125}I] 12** was increased by the introduction of methoxy groups and was slightly different due to the position of methoxy groups, on the order of [**^{125}I]-12** < [**^{125}I]-10** < [**^{125}I]-11**. As shown in Tables 3–5, the liver uptakes in 5, 30, 60, and 120 min post-injection of three *OMe*-modified ^{125}I-TPPs^{+} were also increased on the order of [**^{125}I]-12** < [**^{125}I]-10** < [**^{125}I]-11**. It indicated that the difference of lipophilicity might be the vital factor that influence the pharmacokinetic properties of methoxy groups modified ^{125}I-labeled TPPs cations.

Among three *OMe*-modified ^{125}I-labeled TPPs cations, the *ortho-OMe* modified ^{125}I-TPPs^{+}, [**^{125}I]-10** had the fastest liver clearance, and comparable accumulation in heart, resulted in the highest heart/liver ratio (1.04) at 120 min post-injection. However, [**^{125}I]-10** displayed the highest thyroid uptakes at 60 and 120 min post-injection (1.01 ± 0.02 and 0.92 ± 0.01%ID, respectively), and slight deiodination was also found in the result of in vitro serum stability study. Therefore, further structural optimization is needed to obtain the ^{125}I-TPPs^{+}-based mitochondrial membrane potential targeting probes with improved physicochemical and pharmacokinetic properties. Besides cardiomyocytes, mitochondria are also enriched in many carcinoma cells with mitochondrial dysfunction.[1] Compared with healthy cells, cancer cells have an increase of approximately 60 mV in negative mitochondrial membrane potential ($\Delta\Psi$), which cause a higher accumulation of radiolabeled TPPs^{+} in cancer cells.[24,25] For example, ^{18}F-BnTP has been reported as a potential non-invasive probe to functionally profile mitochondrial membrane potential and mitochondrial heterogeneity within non-small cell lung cancer (NSCLC).[26] Therefore, potential application of these ^{125}I-labeled TPPs^{+} in noninvasive monitoring of mitochondrial membrane potential in cancers can also be considered.

4 | CONCLUSION

In this study, a simple and efficient radioiodination method for the preparation of radioiodine-labeled TPPs^{+} was successfully developed. The method uses Cu_2O/1,10-phenanthroline as the catalyst system, oxygen in the air as the oxidant, triphenylphosphine phenylborate compounds as the labeling precursors, to obtain the radioiodine-labeled TPPs^{+} by a one-step reaction under mild hydrous condition. Four *meta*-^{125}I-labeled-TPPs^{+}, **[^{125}I] 9–[^{125}I] 12** were synthesized in high radiochemical yield (>95%). Results of biological evaluations indicated the four *meta*-^{125}I-labeled-TPPs^{+} could accumulate in the mitochondrial-rich myocardial cells through the mitochondrial membrane potential. Although further structural modification is still needed to improve their pharmacokinetic properties, the highly efficient radioiodination method offers a new strategy to design and prepare novel ^{125}I-labeled-TPPs cations, which lays a prospective foundation for further study and application.

ACKNOWLEDGEMENT

This work was financially supported by the National Natural Science Foundation of China (21976019).

ORCID

Shuyu Shi https://orcid.org/0000-0001-7510-5120
Zelan Liu https://orcid.org/0000-0002-5522-9115
Jie Lu https://orcid.org/0000-0001-6351-0508

REFERENCES

1. Ma C, Xia F, Kelley SO. Mitochondrial targeting of probes and therapeutics to the powerhouse of the cell. *Bioconjug Chem*. 2020;31(12):2650-2667.
2. Lin MT, Beal MF. Mitochondrial dysfunction and oxidative stress in neurodegenerative diseases. *Nature*. 2006;443(7113):787-795.
3. Ballinger SW. Mitochondrial dysfunction in cardiovascular disease. *Free Radic Biol Med*. 2005;38(10):1278-1295.
4. Rosca MG, Hoppel CL. Mitochondrial dysfunction in heart failure. *Heart Fail Rev*. 2013;18(5):607-622.
5. Exner N, Lutz AK, Haass C, Winklhofer FK. Mitochondrial dysfunction in Parkinson's disease: molecular mechanisms and pathophysiological consequences. *EMBO J*. 2012;31(14):3038-3062.
6. Murphy MP. Targeting lipophilic cations to mitochondria. *Biochim Biophys Acta Biomembr*. 2008;1777(7):1028-1031.
7. Azzone GF, Pietrobon D, Zoratti M. Determination of the proton electrochemical gradient across biological membranes. In: Lee CP, ed. *Current Topics in Bioenergetics*. Vol 13. Elsevier; 1984:1-77.
8. Ross MF, Kelso GF, Blaikie FH, et al. Lipophilic triphenylphosphonium cations as tools in mitochondrial bioenergetics and free radical biology. *Biochim Biophys Acta*. 2005;70(2):222-230.
9. Ross MF, Da RT, Blaikie FH, et al. Accumulation of lipophilic dications by mitochondria and cells. *Biochem J*. 2006;400(1):199-208.
10. Kelso GF, Porteous CM, Coulter CV, et al. Selective targeting of a redox-active ubiquinone to mitochondria within cells:

antioxidant and antiapoptotic properties. *J Biol Chem*. 2001;276(7):4588-4596.
11. Smith RAJ, Porteous CM, Coulter CV, Murphy MP. Selective targeting of an antioxidant to mitochondria. *Eur J Biochem*. 1999;263(3):709-716.
12. Filipovska A, Kelso GF, Brown SE, Beer SM, Smith AR, Murphy MP. Synthesis and characterization of a triphenylphosphonium-conjugated peroxidase mimetic: insights into the interaction of ebselen with mitochondria. *J Biol Chem*. 2005;280(25):24113-24126.
13. Madar I, Ravert H, DiPaula A, Du Y, Dannals RF, Becker L. Assessment of severity of coronary artery stenosis in a canine model using the PET agent ^{18}F-fluorobenzyl triphenyl phosphonium: comparison with ^{99m}Tc-tetrofosmin. *J Nucl Med*. 2007;48(6):1021-1030.
14. Shoup TM, Elmaleh DR, Brownell AL, Zhu A, Guerrero JL, Fischman AJ. Evaluation of (4-[^{18}F]fluorophenyl) triphenylphosphonium ion. A potential myocardial blood flow agent for PET. *Mol Imaging Biol*. 2011;13(3):511-517.
15. Kim DY, Kim HJ, Yu KH, Min JJ. Synthesis of [^{18}F]-labeled (2-[2-fluoroethoxy]ethyl)triphenylphosphonium cation as a potential agent for myocardial imaging using positron emission tomography. *Bioorg Med Chem Lett*. 2012;22(1):319-322.
16. Guludec D, Lautamäki R, Knuuti J, Bax JJ, Bengel FM. Present and future of clinical cardiovascular PET imaging in Europe—a position statement by the European Council of Nuclear Cardiology (ECNC). *Eur J Nucl Med Mol*. 2008;35(9):1709-1724.
17. Li J, Lu J, Zhou Y. Mitochondrial-targeted molecular imaging in cardiac disease. *Biomed Res Int*. 2017;2017(2):1-11.
18. Srivastava PC, Knapp FF. [(E)-1-[^{123}I]Iodo-1-penten-5-yl] triphenylphosphonium iodide: convenient preparation of a potentially useful myocardial perfusion agent. *J Med Chem*. 1984;27(8):978-981.
19. Sakai T, Saito Y, Takashima M, Magata Y. Development of radioiodinated lipophilic cationic compounds for myocardial imaging. *Nucl Med Biol*. 2015;42(5):482-487.
20. Yang H, Li Y, Jiang M, Wang J, Fu H. General copper-catalyzed transformations of functional groups from arylboronic acids in water. *Chem A Eur J*. 2011;17(20):5652-5660.
21. Zhang P, Zhuang R, Guo Z, Su X, Chen X, Zhang X. A highly efficient copper-mediated radioiodination approach using aryl boronic acids. *Chem A Eur J*. 2016;22(47):16783-16786.
22. Kim Y-S, Yang C-T, Wang J, et al. Effects of targeting moiety, linker, bifunctional chelator, and molecular charge on biological properties of ^{64}Cu-labeled triphenylphosphonium cations. *J Med Chem*. 2008;51(10):2971-2984.
23. Chen S, Zhao Z, Zhang Y, Fang W, Lu J, Zhang X. Effect of methoxy group position on biological properties of ^{18}F–labeled benzyl triphenylphosphonium cations. *Nucl Med Biol*. 2017;49:16-23.
24. Moura C, Mendes F, Gano L, Santos I, Paulo A. Mono- and dicationic Re(I)/^{99m}Tc(I) tricarbonyl complexes for the targeting of energized mitochondria. *J Inorg Biochem*. 2013;123(8):34-45.
25. Zhou Y, Liu S. ^{64}Cu-labeled phosphonium cations as PET radiotracers for tumor imaging. *Bioconjug Chem*. 2011;22(8):1459-1472.
26. Momcilovic M, Jones A, Bailey ST, et al. In vivo imaging of mitochondrial membrane potential in non-small-cell lung cancer. *Nature*. 2019;575(7782):380-384.

How to cite this article: Shi S, Liu Z, Wu Z, Zhou H, Lu J. Preparation and biological evaluation of radioiodine-labeled triphenylphosphine derivatives as mitochondrial targeting probes. *J Label Compd Radiopharm*. 2021;1–11. https://doi.org/10.1002/jlcr.3910